

Contributions of electron and phonon transport to the thermal conductivity of GdFeCo and TbFeCo amorphous rare-earth transition-metal alloys

Patrick E. Hopkins, Manli Ding, and Joseph Poon

Citation: *J. Appl. Phys.* **111**, 103533 (2012); doi: 10.1063/1.4722231

View online: <http://dx.doi.org/10.1063/1.4722231>

View Table of Contents: <http://jap.aip.org/resource/1/JAPIAU/v111/i10>

Published by the [American Institute of Physics](http://www.aip.org).

Related Articles

CaLi-based bulk metallic glasses with multiple superior properties
Appl. Phys. Lett. **93**, 171907 (2008)

Transport properties of Ti-Zr-Ni quasicrystalline and glassy alloys
J. Appl. Phys. **104**, 063705 (2008)

High frequency dynamics in liquid nickel: An inelastic x-ray scattering study
J. Chem. Phys. **128**, 234502 (2008)

Temperature effect of the local structure in liquid Sb studied with x-ray absorption spectroscopy
J. Chem. Phys. **128**, 224501 (2008)

Noncontact measurement of thermal conductivity of liquid silicon in a static magnetic field
Appl. Phys. Lett. **90**, 094102 (2007)

Additional information on J. Appl. Phys.

Journal Homepage: <http://jap.aip.org/>

Journal Information: http://jap.aip.org/about/about_the_journal

Top downloads: http://jap.aip.org/features/most_downloaded

Information for Authors: <http://jap.aip.org/authors>

ADVERTISEMENT



AIP Advances

Now Indexed in Thomson Reuters Databases

Explore AIP's open access journal:

- Rapid publication
- Article-level metrics
- Post-publication rating and commenting

Contributions of electron and phonon transport to the thermal conductivity of GdFeCo and TbFeCo amorphous rare-earth transition-metal alloys

Patrick E. Hopkins,^{1,a)} Manli Ding,² and Joseph Poon²¹*Department of Mechanical and Aerospace Engineering, University of Virginia, Charlottesville, Virginia 22904, USA*²*Department of Physics, University of Virginia, Charlottesville, Virginia 22904, USA*

(Received 1 April 2012; accepted 27 April 2012; published online 30 May 2012)

We experimentally investigate the electron and phonon contributions to the thermal conductivity of amorphous GdFeCo and TbFeCo thin films. These amorphous rare-earth transition-metal (RE-TM) alloys exhibit thermal conductivities that increase nearly linearly with temperature from 90 to 375 K. Electrical resistivity measurements show that this trend is due to an increase in the electron thermal conductivity over this temperature range and a relatively constant phonon contribution to thermal conductivity. We find that at low temperatures (~ 90 K), the phonon systems in these amorphous RE-TM alloys contribute $\sim 70\%$ to thermal conduction with a decreasing contribution as temperature is increased. © 2012 American Institute of Physics. [<http://dx.doi.org/10.1063/1.4722231>]

I. INTRODUCTION

Amorphous rare-earth transition-metal (RE-TM) alloys represent an interesting class of materials to study the influence of non-crystalline order on various physical properties. In their electronic properties, for example, transition-metal spin value, exchange interaction, and the band structure are drastically different compared to their crystalline counterpart.¹ Due to fluctuations in the local structure, the amorphous state also exhibits a much lower Curie temperature resulting in different magnetic responses.² However, the thermal properties of amorphous RE-TM alloys are relatively unknown.

In amorphous dielectrics, the thermal conductivity above ~ 100 K is well described by the minimum thermal conductivity model originally proposed by Einstein³ and later modified by others to include heat transport by a broader spectrum of vibrational modes.⁴⁻⁶ However, this picture does not fully describe the thermal transport in amorphous metals due to the electron contribution to thermal conductivity and the strong electron-phonon coupling effects.⁷ Several previous works have examined the thermal conductivity of Zr-, Ni-, or Cu-based metallic glasses.⁸⁻¹² In general, the thermal conductivity of metallic glasses increases with temperature and has a much larger contribution from the phonon system than in typical metals (ranging from 20% to 50% at room temperature).^{8,11} The thermal transport properties of amorphous RE-TM alloys have not been thoroughly investigated, to the best of our knowledge. Amorphous RE-TM alloys have received much attention with respect to their application as magneto-optical recording media with GdFeCo and TbFeCo alloys being the most promising candidates.^{1,13-16} These recording systems utilize the heating effect of a laser beam for storing digital information in a multilayer disk, and the storage and operation of these systems depend immensely on the thermal properties

of the disk layers. However, the data for the thermal conductivity of GdFeCo and TbFeCo alloys are relatively nonexistent and only estimates are available at room temperature.¹⁷ This severely limits not only the progress of magneto-optical recording technology but also the progress in understanding the thermophysics of amorphous RE-TM alloys.

In response, we experimentally investigate the electron and phonon contributions to thermal conductivity of GdFeCo and TbFeCo amorphous thin films from 90 to 375 K. We use time domain thermoreflectance (TDTR) to measure the thermal conductivities of these films and we calculate the electron contribution to thermal conductivity from our electrical resistivity measurements via the Weidemann-Franz Law. From this, we infer the phonon contribution to the overall thermal conductivity of these amorphous RE-TM alloy films. We find that the phonon contribution to the thermal conductivity (κ_p) is relatively constant with temperature; this is similar to previously measured pure metallic glasses, yet glasses with non-metal impurities show an increasing phonon contribution to thermal conductivity with temperature. Furthermore, we find that the electron contribution to the thermal conductivity (κ_e) of our amorphous RE-TM alloy films increases with temperature. We find that at low temperatures (~ 90 K), the phonon systems in these amorphous RE-TM alloys contribute $\sim 70\%$ to thermal conduction which drops at room temperature due to the increase in κ_e .

II. EXPERIMENTAL DETAILS

The 260 nm Gd₂₁Fe₇₂Co₇ (GdFeCo) and 300 nm Tb₂₁Fe₇₃Co₆ (TbFeCo) films are grown on single crystalline silicon substrates via RF sputtering. The films are capped with ~ 5 nm of MgO to prevent oxidation. We measured the film composition using inductively coupled plasma-mass spectrometry after chemically dissolving the films, as confirmed by x-ray fluorescence using peak ratios. We confirm that the films are fully amorphous with transmission electron microscopy (TEM). Figure 1 shows an example of a

^{a)}Electronic mail: phopkins@virginia.edu.

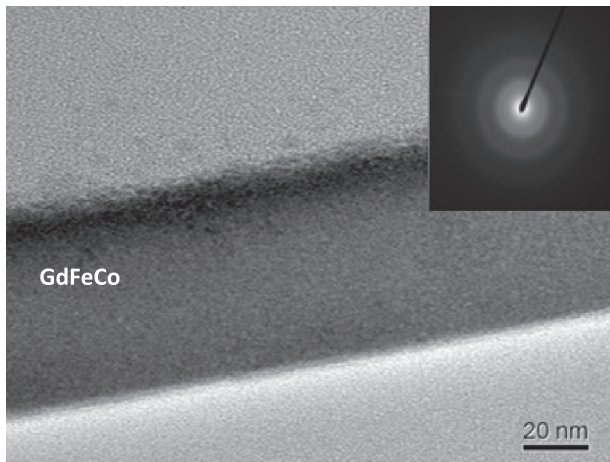


FIG. 1. Cross-section bright field TEM of a GdFeCo film. (Inset) Corresponding electron diffraction pattern, indicating the lack of crystallinity.

cross-section bright field TEM of a GdFeCo film. The inset shows the corresponding electron diffraction pattern, indicating the lack of crystallinity.

The thermal conductivities of the amorphous RE-TM alloy films are measured with TDTR.¹⁸ TDTR and appropriate analyses accounting for pulse accumulation when using a Ti:sapphire oscillator have been detailed by several groups previously.^{19–22} We note that TDTR is ideal for measuring thermal properties of thin films due to its picosecond temporal resolution and high heating modulation frequency leading to nanoscale spatial resolution. Numerous papers have discussed the sensitivities, calibrations, and advantages of measuring thermal transport properties in both bulk and nanosystems with TDTR.^{18–26} Since this work focuses on the underlying physics contributing to thermal transport of RE-TM alloys, we limit our discussion of TDTR to only the specifics discussed below, but refer the reader to the above referenced papers, and references therein, for more details concerning TDTR.

In our specific set up at the University of Virginia, we double the wavelength of the pump path to 400 nm to assist with optical filtering of the pump light giving us improved signal to noise of rough surfaces. For this study, we modulate the pump path at 11.39 MHz and monitor the ratio of the in-phase to out-of-phase signal of the probe beam from a lock-in amplifier ($-V_{in}/V_{out}$). Our pump and probe spots are focused to $\sim 22 \mu\text{m}$ and $\sim 13 \mu\text{m}$ radii, respectively, at the sample surface. We take a total of five TDTR measurements on the various films at each temperature from 90 to 375 K. We control the temperature of the samples in a cryostat with optical access that is kept under vacuum (pressures less than 1.0 mTorr). The amorphous RE-TM alloy samples are coated with $\sim 90 \text{ nm}$ of Al for the TDTR measurements; the exact thicknesses of the Al film are determined during each measurement with picosecond ultrasonics.²⁷ For the TDTR analysis, we assume literature values for the heat capacities of the Al and Si.^{28,29} The thermal conductivity of the Al is approximated from the electrical resistivity measurements,²¹ although over the time delay during our TDTR measurements, we are relatively insensitive to the thermal

conductivity of the Al. The thermal conductivity of the Si substrate is assumed as that of bulk,³⁰ although we are insensitive to the substrate thermal properties due to the thickness of the amorphous RE-TM alloy films and their relatively low thermal conductivities. For this reason, we are also relatively insensitive to the thermal boundary conductance between the amorphous RE-TM alloys and the Si substrate. This leaves the only thermophysical properties that need to be determined as the thermal conductivity and heat capacity of the amorphous RE-TM alloy and the thermal boundary conductance between the Al and amorphous RE-TM alloy.

In practice, a single TDTR data set can independently determine both the thermal boundary conductance between the Al transducer and the amorphous RE-TM alloy given the heat capacity of the amorphous RE-TM alloy. The heat capacity of GdFeCo and TbFeCo have been reported at room temperature and vary anywhere from 2.3 to 3.1 $\text{MJ m}^{-3} \text{K}^{-1}$ (Refs. 13, 16, 32, and 33). We therefore specify the room temperature heat capacity of the GdFeCo and TbFeCo films as 2.7 $\text{MJ m}^{-3} \text{K}^{-1}$ and account for the uncertainty in this value in our thermal conductivity determinations as discussed later. To determine the heat capacity at the various temperatures, we assume a Debye model for the phonon system in the amorphous RE-TM alloys and calculate the heat capacity at the temperatures of interest in this study. These calculations require the sound speed and the atomic density of the amorphous RE-TM alloys. We measure the speed of sound with picosecond ultrasonics directly applied to the sample (i.e., a portion without Al coating);²⁷ we measure the longitudinal speed of sound as $4200 \pm 210 \text{ m s}^{-1}$ and $3900 \pm 190 \text{ m s}^{-1}$ for the GdFeCo and TbFeCo films, respectively. We determine the transverse sound speeds by calculating the square root of the ratio of the shear modulus to the bulk modulus of GdFeCo or TbFeCo, and multiplying this value by the longitudinal sound speed determined from picosecond ultrasonics. We determine the moduli of the RE-TM alloys by calculating the weighted reciprocal mean of the shear moduli of the elements in the alloys.³⁴ From this, we determine the transverse speeds of sound as 3050 m s^{-1} and 2820 m s^{-1} for the GdFeCo and TbFeCo films, respectively. We adjust the atomic density in the calculations of the heat capacity until the room temperature value of our calculations is 2.7 $\text{MJ m}^{-3} \text{K}^{-1}$ for both of the alloys. This leads to GdFeCo and TbFeCo atomic densities of 7.4 and 7.1 $\times 10^{28} \text{ m}^{-3}$, respectively. Note that this is in acceptable agreement with previously reported values for the atomic density of TbFeCo ($6.5 \times 10^{28} \text{ m}^{-3}$ —Ref. 15) and calculations of atomic density based on the density of the elemental constituents and a rule of mixing ($\sim 6 \times 10^{28} \text{ m}^{-3}$). With our calculated estimates of the heat capacities, we then fit the TDTR thermal model to the experimental data with the only free parameters being the thermal boundary conductance between the Al film and the amorphous RE-TM alloy and the thermal conductivity of the amorphous RE-TM alloy. We find in general that the fit is relatively insensitive to the thermal boundary conductance between the Al transducer and the amorphous RE-TM alloy sample due to the relatively low thermal conductivity of the alloys compared to the relatively high thermal boundary conductance.

III. RESULTS AND DISCUSSION

Figure 2 shows the measured thermal conductivities of the amorphous RE-TM alloy films as a function of temperature determined via TDTR. The error bars in these data represent the uncertainties due to repeatability in the measurements, the Al transducer thickness, and the amorphous RE-TM alloy heat capacity. We determine the Al film thickness to within 3.0 nm via picosecond ultrasonics. Therefore, the majority of the uncertainty in κ is due to the uncertainty in the assumed heat capacity, which we take as 15% for all temperatures based on the previously reported values for heat capacity of GdFeCo and TbFeCo, as discussed earlier. The thermal conductivities of both the GdFeCo and TbFeCo films increase nearly linearly with temperature. This is a similar trend as to what has been observed in metallic glasses previously.^{8–12} For comparison, we show the thermal conductivity of a pure metallic glass ($\text{Zr}_{55}\text{Al}_{10}\text{Cu}_{30}\text{Ni}_5$ (Ref. 12)), metallic glasses with non-metallic

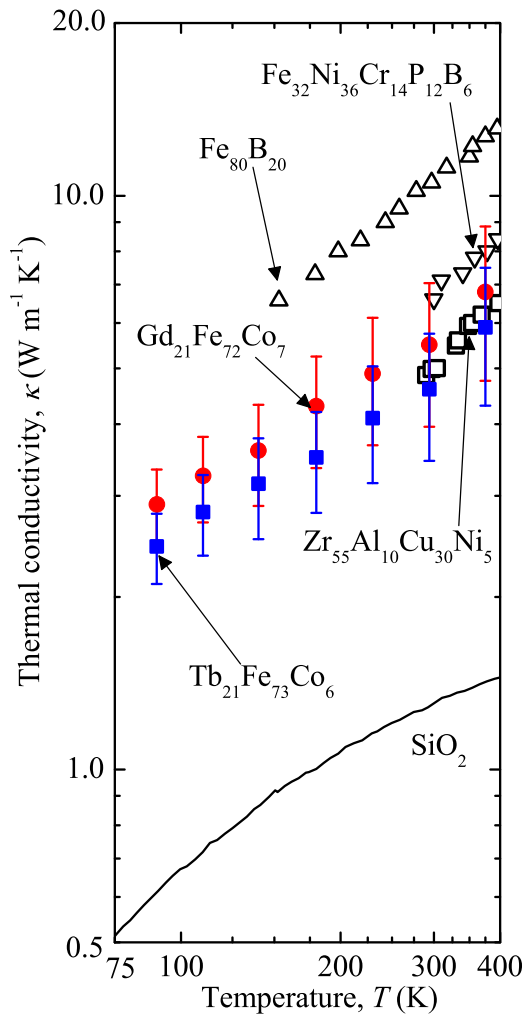


FIG. 2. Thermal conductivity of the GdFeCo and TbFeCo films ($\text{Gd}_{21}\text{Fe}_{72}\text{Co}_7$ —filled circles and $\text{Tb}_{21}\text{Fe}_{73}\text{Co}_6$ —filled squares) measured with TDTR. The thermal conductivities of these amorphous RE-TM alloys increase, nearly linearly, with temperature. This same trend is observed in other metallic glasses, for example, $\text{Fe}_{80}\text{B}_{20}$ (Ref. 9—upward open triangles), $\text{Fe}_{32}\text{Ni}_{36}\text{Cr}_{14}\text{P}_{12}\text{B}_6$ (Ref. 9—downward open triangles), and $\text{Zr}_{55}\text{Al}_{10}\text{Cu}_{30}\text{Ni}_5$ (Ref. 12—open squares). For comparison, we also plot SiO_2 glass (Ref. 31—solid line) which increases with temperature with trends similar to the temperature trends in the phononic heat capacity.

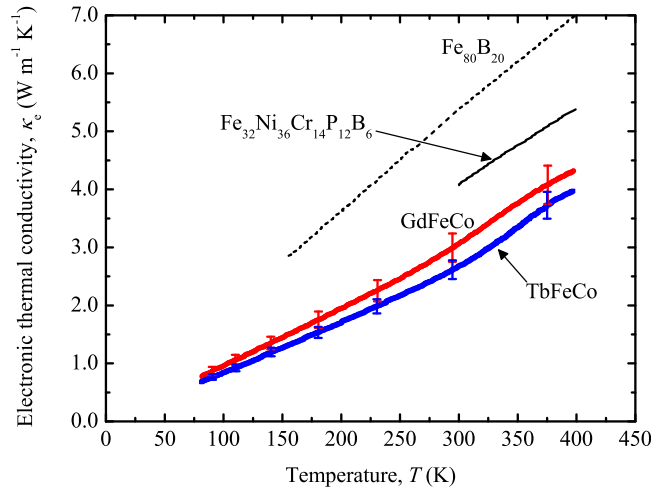


FIG. 3. Electron contribution to thermal conductivity of the amorphous RE-TM alloy films. This thermal conductivity component was determined via electrical resistivity measurements and the Wiedemann-Franz Law. Both amorphous samples exhibit a linear κ_e with temperature. We estimate the relative uncertainties in these electrical resistivity measurements by considering the effects of contact size and placement along with the sample geometry.³⁵ These uncertainties are represented by the error bars shown at select temperatures in the GdFeCo and TbFeCo data, and correspond to 8.1% and 6.2%, respectively. We also plot the reported electron contributions to the thermal conductivities of the metallic glasses with non-metal impurities ($\text{Fe}_{80}\text{B}_{20}$ (dashed line) and the $\text{Fe}_{32}\text{Ni}_{36}\text{Cr}_{14}\text{P}_{12}\text{B}_6$ (solid line)) reported in Ref. 9, which also show similar temperature trends in electron thermal conductivity.

constituents ($\text{Fe}_{80}\text{B}_{20}$ (Ref. 9) and $\text{Fe}_{32}\text{Ni}_{36}\text{Cr}_{14}\text{P}_{12}\text{B}_6$ (Ref. 9)), and SiO_2 glass (Ref. 31). The metallic glasses all exhibit similar temperature trends in thermal conductivity, increasing more linearly as compared to the nonmetallic SiO_2 which increases with temperature trends similar to the phononic heat capacity.

To understand the origin of these temperature trends in the thermal conductivity of amorphous RE-TM alloys, we measure the electrical resistivity from 80 to 400 K with a standard four-point van der Pauw configuration in a Quantum Design cryogen-free vibrating sample magnetometer (VersaLab). From these measurements, we calculate the electron contribution to the thermal conductivity via the Wiedemann-Franz Law. For the GdFeCo and TbFeCo films, κ_e is plotted in Fig. 3. The electronic thermal conductivities of both films exhibit nearly linear trends with temperature. This linear trend in κ_e has also been observed in the metallic glasses with non-metallic constituents shown in Fig. 2 ($\text{Fe}_{80}\text{B}_{20}$ (Ref. 9) and $\text{Fe}_{32}\text{Ni}_{36}\text{Cr}_{14}\text{P}_{12}\text{B}_6$ (Ref. 9)).

To quantify this, we calculate the phonon contribution to thermal conductivity by $\kappa_p = \kappa - \kappa_e$, where κ is determined from the TDTR measurements (Fig. 2) and κ_e is determined from the electrical resistivity measurements (Fig. 3). We plot κ_p for the amorphous RE-TM alloy films in Fig. 4. The phonon thermal conductivity is relatively constant over the temperature range of interest. The slight increase that is observed in the mean values is hard to conclusively discern beyond the relative uncertainties in the calculations, which propagates from the relative uncertainties in the TDTR and electrical resistivity data that were previously discussed. This constant κ_p has been observed in pure amorphous metals previously.¹² However, the amorphous metals with boron or phosphorous ($\text{Fe}_{80}\text{B}_{20}$ and $\text{Fe}_{32}\text{Ni}_{36}\text{Cr}_{14}\text{P}_{12}\text{B}_6$ (Ref. 9))

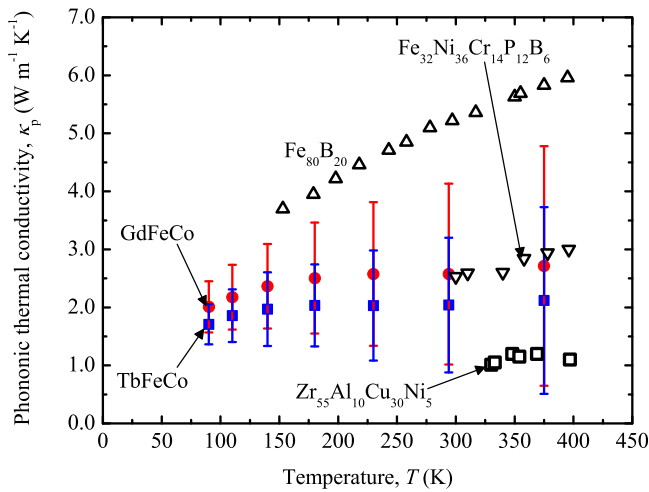


FIG. 4. Calculated phonon contribution to the thermal conductivity of the amorphous RE-TM alloys based on the data presented in Figs. 2 and 3. The error bars represent the relative uncertainties calculated from adding the relative uncertainties shown in Figs. 2 and 3 in quadrature. The phonon thermal conductivity is relatively constant over the temperature range of interest. This constant phonon contribution to thermal conductivity has been observed in previous measurements of pure metallic glasses ($Zr_{55}Al_{10}Ni_5Cu_{30}$ (Ref. 12—open squares)). However, metallic glasses with non-metal constituents exhibit an increase in κ_p with temperature ($Fe_{80}B_{20}$ (upward open triangles—Ref. 9) and $Fe_{32}Ni_{36}Cr_{14}P_{12}B_6$ (downward open triangles—Ref. 9).

show an increase in κ_p with temperature, unlike the pure amorphous metals. The reason for this is currently unclear, but could be due to a stiffening of the bonds with non-metallic inclusions that leads to an increase in the Debye temperature, and thereby an increasing trend in phonon thermal conductivity compared to the pure metallic glasses.

Based on the data in Figs. 3 and 4, the percent phonon contribution decreases with increasing T where the electron contribution increases with increasing T . We find that the percent contribution of the phonon system to thermal conductivity is $\sim 70\%$ at 90 K and decreases to a still significant contribution at room temperature and above. At low temperatures, the phonons contribute more to the thermal conductivity of the amorphous RE-TM alloys than the electrons, a phenomenon that is not typical in most metals.

IV. CONCLUSIONS

In summary, we have investigated the electron and phonon contributions to the thermal conductivity of amorphous GdFeCo and TbFeCo thin films, a class of amorphous RE-TM alloys that is extremely important for the continued development of magneto-optical recording devices. The thermal conductivities exhibit a nearly linear increase with temperature from 90 to 375 K, which is due to the increase in electron thermal conductivity and a relatively constant phonon contribution to thermal conductivity. We find that at low temperatures (~ 90 K), the phonon systems in these amorphous RE-TM alloys contribute $\sim 70\%$ to thermal conduction which decreases at higher temperatures due to the increase in the electronic thermal conductivity.

ACKNOWLEDGMENTS

The authors are grateful for support from Defense Threat Reduction Agency Grant No. HDTRA1-11-1-0024 and the National Science Foundation Grant Nos. CBET 0748009 and 1134311.

- ¹P. Hansen, C. Clausen, G. Much, M. Rosenkranz, and K. Witter, *J. Appl. Phys.* **66**, 756 (1989).
- ²C. C. Tsuei and H. Lilienthal, *Phys. Rev. B* **13**, 4899 (1976).
- ³A. Einstein, *Ann. Phys.* **35**, 679 (1911).
- ⁴G. A. Slack, in *Solid State Physics: Advances in Research and Applications*, edited by H. Ehrenreich, F. Seitz, and D. Turnbull (Academic, New York, 1979), Vol. 34, pp. 1–73.
- ⁵D. G. Cahill, S. K. Watson, and R. O. Pohl, *Phys. Rev. B* **46**, 6131 (1992).
- ⁶P. E. Hopkins and T. Beechem, *Nanoscale Microscale Thermophys. Eng.* **14**, 51 (2010).
- ⁷J. Jackle and K. Frobose, *J. Phys. F: Met. Phys.* **10**, 471 (1980).
- ⁸C. L. Choy, K. W. Tong, H. K. Wong, and W. P. Leung, *J. Appl. Phys.* **70**, 4919 (1991).
- ⁹C. L. Choy, W. P. Leung, and Y. K. Ng, *J. Appl. Phys.* **66**, 5335 (1989).
- ¹⁰A. Jezowski, J. Mucha, and G. Pompe, *J. Phys. D: Appl. Phys.* **20**, 1500 (1987).
- ¹¹N. C. Shukla, H. H. Liao, J. T. Abiade, F. Liu, P. K. Liaw, and S. T. Huxtable, *Appl. Phys. Lett.* **94**, 081912 (2009).
- ¹²M. Yamasaki, S. Kagao, and Y. Kawamura, *Scr. Mater.* **53**, 63 (2005).
- ¹³M. K. Loze, C. D. Wright, R. Atkinson, and W. W. Clegg, *J. Magn. Magn. Mater.* **222**, 379 (2000).
- ¹⁴M. H. Kryder, *J. Appl. Phys.* **57**, 3913 (1985).
- ¹⁵W. Hwang and H. D. Shieh, *J. Appl. Phys.* **81**, 2745 (1997).
- ¹⁶Y. Tanaka, M. Kurebayashi, T. Kohashi, Y. Murakami, and S. Yonezawa, *Appl. Opt.* **37**, 2699 (1998).
- ¹⁷S. S. Kim, Y. M. Ahn, K. G. Lee, and B. L. Gill, *IEEE Trans. Magn.* **32**, 4093 (1996).
- ¹⁸D. G. Cahill, K. E. Goodson, and A. Majumdar, *J. Heat Transfer* **124**, 223 (2002).
- ¹⁹D. G. Cahill, *Rev. Sci. Instrum.* **75**, 5119 (2004).
- ²⁰A. J. Schmidt, X. Chen, and G. Chen, *Rev. Sci. Instrum.* **79**, 114902 (2008).
- ²¹P. E. Hopkins, J. R. Serrano, L. M. Phinney, S. P. Kearney, T. W. Grasser, and C. T. Harris, *J. Heat Transfer* **132**, 081302 (2010).
- ²²P. E. Hopkins, B. Kaehr, L. M. Phinney, T. P. Koehler, A. M. Grillet, D. Dunphy, F. Garcia, and C. J. Brinker, *J. Heat Transfer* **133**, 061601 (2011).
- ²³A. Schmidt, M. Chiesa, X. Chen, and G. Chen, *Rev. Sci. Instrum.* **79**, 064902 (2008).
- ²⁴P. M. Norris, A. P. Caffrey, R. J. Stevens, J. M. Klopff, J. T. McLeskey, and A. N. Smith, *Rev. Sci. Instrum.* **74**, 400 (2003).
- ²⁵P. M. Norris and P. E. Hopkins, *J. Heat Transfer* **131**, 043207 (2009).
- ²⁶P. M. Norris, J. L. Smoyer, J. C. Duda, and P. E. Hopkins, *J. Heat Transfer* **134**, 020910 (2012).
- ²⁷C. Thomsen, J. Strait, Z. Vardeny, H. J. Maris, J. Tauc, and J. J. Hauser, *Phys. Rev. Lett.* **53**, 989 (1984).
- ²⁸Y. S. Touloukian, R. W. Powell, C. Y. Ho, and P. G. Klemens, *Thermophysical Properties of Matter—Specific Heat: Nonmetallic Solids* (IFI/Plenum, New York, 1970), Vol. 5.
- ²⁹Y. S. Touloukian and E. H. Buyco, *Thermophysical Properties of Matter—Specific Heat: Metallic Elements and Alloys* (IFI/Plenum, New York, 1970), Vol. 4.
- ³⁰Y. S. Touloukian, R. W. Powell, C. Y. Ho, and P. G. Klemens, *Thermophysical Properties of Matter—Thermal Conductivity: Nonmetallic Solids* (IFI/Plenum, New York, 1970), Vol. 2.
- ³¹D. G. Cahill, *Rev. Sci. Instrum.* **61**, 802 (1990).
- ³²X. Xun, C. Peng, and M. Mansuripur, *Appl. Opt.* **41**, 4596 (2002).
- ³³H. Ide, T. Toda, F. Kirino, T. Maeda, F. Kugiyu, S. Mita, and K. Shigematsu, *Jpn. J. Appl. Phys.* **32**, 5342 (1993).
- ³⁴S. J. Poon and K. Limtragoon, *J. Appl. Phys.* **110**, 114306 (2011).
- ³⁵D. W. Koon, *Rev. Sci. Instrum.* **60**, 271 (1989).